Prostate Cancer Detection Based on Three Dimensional Sonoelastography

B.Castaneda, K. Hoyt, M. Zhang, D. Pasternack, L. Baxter, P. Nigwekar, A. di Sant'Agnese,
J. Joseph, J. Strang, D.J. Rubens, and K.J. Parker
Rochester Center for Biomedical Ultrasound
University of Rochester
Rochester, NY, USA

Abstract—In this paper, we evaluate the performance of sonoelastography for prostate cancer detection. Ultrasound (US) B-mode and sonoelastographic volumes were acquired from five prostate glands *ex vivo*. Additionally, one more gland was imaged *in vivo* using a transrectal US probe. Semi-automatic algorithms were used to segment the surface of the gland from the B-mode volume and the tumors from sonoelastographic data. To assess the detection performance, three dimensional (3D) sonoelastographic findings were compared in size and position to 3D histological data. Sonoelastography detected seven out of nine cancers in the *ex vivo* prostate glands and two out of three malignant masses in the *in vivo* experiment. Overall, 3D sonoelastography has shown potential for prostate cancer detection albeit based on limited data.

Keywords- Elasticity imaging; three-dimensional sonoelastography; prostate cancer detection

I. INTRODUCTION

Prostate cancer is the most prevalent type of cancer in men, and it is second only to lung cancer in mortality among adult males. In the United States, the number of new cases diagnosed with prostate cancer in 2007 is calculated as 218,890, whereas the number of estimated deaths is 27,000 [1]. Early and accurate detection is a priority in order not only to reduce mortality but also to prevent side effects from local symptoms such as bleeding, urinary tract obstruction and development of metastases.

Current prostate cancer diagnosis relies on a combination of digital rectal examination (DRE), screening based on prostate specific antigen levels (PSA) and biopsy guided by transrectal ultrasound (TRUS) imaging. These methods have shown shortcomings in accuracy and specificity and, therefore, new diagnostic tools are needed. DRE is limited anatomically to the posterior of the gland and may miss cancers in other regions [2]. Also, PSA levels can be increased not only by cancer but other conditions such as hyperplasia and prostatic inflammation [3]. To further complicate prostate cancer detection, TRUS imaging fails to discriminate isoechoic cancers making random biopsies necessary [4]. However, a high number of biopsies per patient yields a low number of cancers detected with this procedure [5].

DRE is based on the premise that pathological processes produce changes in tissue mechanical properties. Under this rationale, imaging the elastic properties of biological tissues

has become an area of active research [6,7,8] with some efforts focused on prostate cancer detection [5,9,10,11]. In particular, sonoelastography is a tissue elasticity imaging technique that estimates the amplitude response of tissues under harmonic mechanical excitation using ultrasonic Doppler techniques [12]. Due to a relationship between particle vibrational response and received Doppler spectral variance [13], the amplitude of low frequency shear waves propagating in tissue can be visualized in real-time using sonoelastography to detect regions of abnormal stiffness [14].

In this paper, we present *ex vivo* and *in vivo* results from an on-going study at the University of Rochester to evaluate the performance of sonoelastography for prostate cancer detection. Specifically, we introduce the use of a semi-automatic algorithm to determine the size and position of tumors from three dimensional (3D) sonoelastographic data, which are compared to histological volumes.

II. METHODS

The *ex vivo* and *in vivo* studies involving human prostate glands presented in this paper were approved by the Institutional Review Board of the University of Rochester Medical Center and compliant with the Health Insurance Portability and Accountability Act. In all cases, it was verified that the patient was not treated with radiation or hormonal therapies which alter the gland stiffness and the amount of residual tumor.

A. Ex vivo experiments

Human prostate glands were received after radical prostatectomy and embedded in a 10.5% gelatin (300 Bloom Pork Gelatin, Gelatin Innovations Inc., Schiller Park, IL, USA) bowl-shaped mold. Vibration was provided by two parallel rigid metal strips positioned underneath the mold. The strips had a rectangular cross section (90 mm in length, 6 mm in width and 7 mm in height) and were connected to an external piston (Vibration Test Systems, Aurora, OH, USA). Input signals to the piston were provided by a harmonic waveform generator (Model 3511A Pragmatic Instruments, San Diego, CA, USA) after amplification (Model 2706, Brüel & Kjaer, Naerum, Denmark). The metals strips were vibrated at a combination of low frequencies (105, 140, 175 and 210 Hz) to minimize imaging artifacts resulting from reflections from the boundaries of the mold [15]. Co-registered sonoelastographic

and B-mode ultrasound (US) volumes were acquired using a modified Logiq 9 US scanner (General Electric Medical Systems, Milwaukee, WI, USA). Images were obtained at 1-mm spacing in the longitudinal direction (i.e. prostate apex to base) by mounting a M12L linear array probe on a motorized track (Velmex, Bloomfield, NY, USA). The image plane was normal to the long axis of the metal strips.

After imaging, the specimen was weighted and measured to determine the maximum length from apex to base, transversely and anteroposteriorly. A landmark device, which consisted of two sets of four 3-mm-diameter mating metal prongs, was inserted longitudinally into the specimen to provide fiducial markers. After fixation, the gland was measured to assess shrinkage, sliced into 4-mm-thick sections from the apex to the base, and digitally photographed. Tissues were then transferred to cassettes and embedded in paraffin (Paraplast, Sherwood Medical, St. Louis, MO, USA). The tissue was sliced further into 5-μm-thick sections and placed on glass slides. The microscopic whole-mount sections were examined by a pathologist who was blinded to the results from sonoelastography. Areas of carcinoma were outlined with a color marking pen. Subsequently, a histological volume was created by aligning the digital photographs of each histological slide using the holes from the landmark device as a reference. The volume was scaled to compensate for shrinkage.

Discrete dynamic contours were used to outline the boundary of the prostate gland in each of the B-mode US images resulting in a 3D representation of the surface of the gland [16]. Deficits in the sonoelastographic images (indicative of a stiff or cancerous region) were segmented using a semi-automatic algorithm presented in [17] but extended to the 3D domain. The algorithm was initialized by subjectively selecting the center of the deficit. Subsequently, the algorithm performed a combination of fast marching and level set methods to establish the final segmentation of the lesion. This process was repeated for each deficit found in the sonoelastographic volume. Information from the co-registered images was fused creating a volume showing the deficits found in the prostate gland in 3D. Rigid registration of the US and pathology volumes was achieved by using the surface of the gland as a marker [18]. To assess the detection performance, 3D sonoelastographic findings were compared in size and position to 3D histology. For tumors to match, the relative average diameter in sonoelastographic images with respect to histological images had to be between 50% and 150%, and the tumor centers had to be less than 8 mm apart. These criteria were selected to compensate for problems during registration and for the coarse sampling in the histological volume.

B. In vivo case

The patient underwent a TRUS examination the day prior to his scheduled radical prostatectomy. A magnetic tracking device (MiniBird, Ascension Technologies, Burlington, VA, USA) was mounted on the TRUS probe [18]. This device enabled the reconstruction of 3D US B-mode and sonoelastographic volumes of the prostate gland. The external vibration was induced by a specially designed plate using two mechanical actuators (Buttkicker Concert, The Guitammer Company Inc., Westerville, Ohio, USA) each driven by a low

frequency harmonic signal (70 Hz). After surgery, a histological volume was reconstructed and registered to the US images following the protocol detailed in section IIA.

III. RESULTS

Sonoelastography found 10 deficits in the five *ex vivo* glands that were examined. Seven of the deficits corresponded to cancerous masses and three were false positives. Two tumors were missed entirely representing false negatives. The average diameters of the detected tumors were 10.2 ± 2.4 mm and 10.7 ± 3.7 mm as measured from sonoelastographic and histological images, respectively. The two undetected tumors measured 5.3 and 4.0 mm in diameter. Fig. 1 illustrates a representative *ex vivo* case comparing findings from imaging and histology. The sonoelastographic image depicts a tumor in the left posterior part of the gland as verified by histology. Note that the same tumor is not visible in the corresponding US B-mode image. Reconstructed histological and US volumes for the same prostate case are depicted in Fig. 2. It is observed that the deficit found in the sonoelastographic volume overlaps with the tumor outlined by the pathologist.

For the *in vivo* prostate case, histological images showed three cancerous masses. Two of them were detected with an average diameter of 6.9 mm and 10.1 mm measured from sonoelastographic data versus 4.8 mm and 9.7 mm measured from histology. The undetected tumor had a diameter of 6 mm. Fig. 3 presents a representative image for this case. Specifically, a B-mode US scan and the corresponding sonoelastographic image show a sagital view of the gland *in vivo*. Sonoelastography depicts a tumor in the middle of the image close to the apex of the gland in agreement with the hypoechoic mass seen on US B-mode.

IV. DISCUSSION

The false positives found in these results may be related to the presence of benign conditions, which can be stiffer than normal tissue, e.g. benign prostate hyperplasia and calcification clusters [19], or to imaging artifacts known as modal patterns. These artifacts appear due to the destructive interference between the shear waves created by the vibration sources and their reflection from boundaries of the gelatin mold. Although multiple-frequency signals were used to minimize this effect, they are not sufficient to eradicate it. In order to avoid these sources of false positives, the *ex vivo* experimental setup needs to be adjusted to either minimize modal patterns or determine their presence. Also, studies into the viscoelastic properties of benign conditions are needed.

The *in vivo* experiment showed high contrast sonoelastographic images. Furthermore, these images are less affected by modal patterns. This can be attributed to the heterogeneous nature of tissue and the lack of strong boundary reflections. However, coupling of externally induced mechanical vibrations to the prostate tissue remains the main challenge to obtain high-quality results *in vivo*.
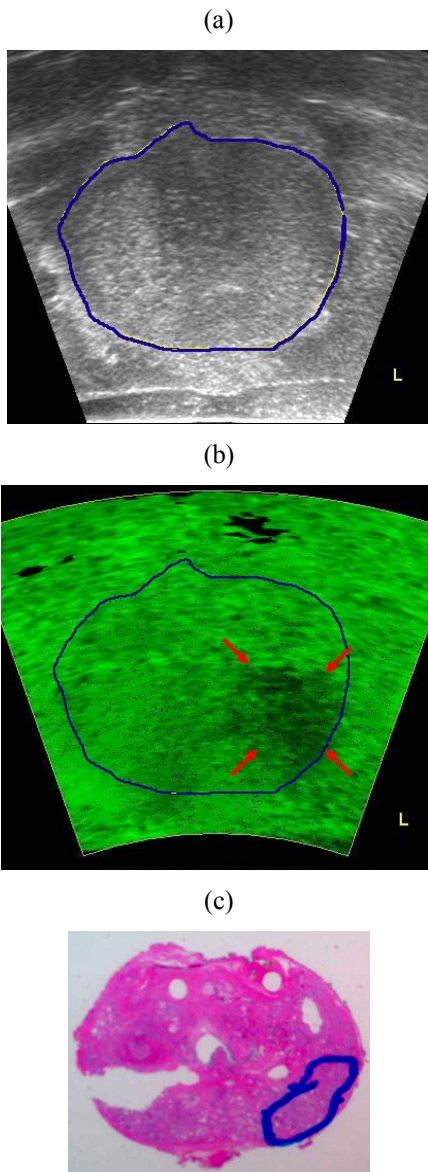
(a)

(b)

(c)

Figure 1.   Corresponding (a) B-mode US image and (b) sonoelastographic image from an *ex vivo* prostate study. Although not visualized in B-mode US, a cancerous mass (red arrows) is depicted in the sonoelastographic image as verified by (c) the histological image (blue outine).
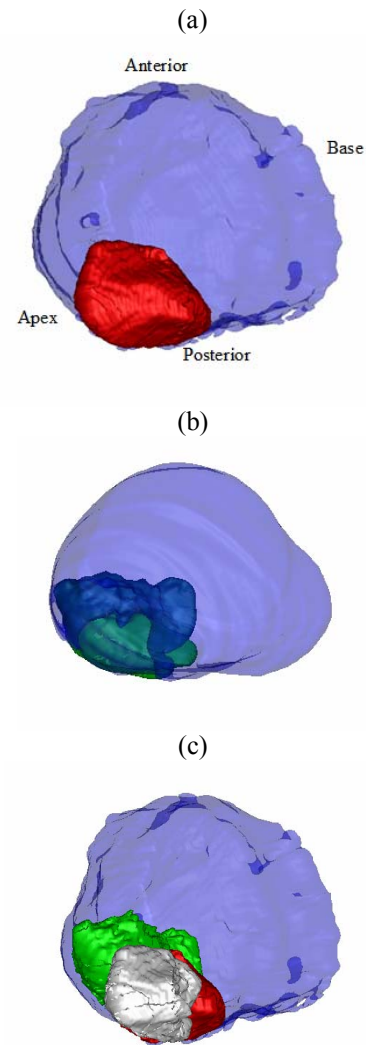
(a)

(b)

(c)

Figure 2.   Volumes reconstructed from (a) histological images and (b) ultrasound images. The tumor found by the pathologist is depicted in red. The deficit found by sonoelastography is shown in green. The fusion of both volumes is illustrated in (c). The overlap of the tumors from sonoelastography and histology is presented in white.

The capability of sonoelastography to find cancerous masses depends on the size and elastic contrast of the tumor in comparison with the normal surrounding tissue [14]. Small size and low contrast represent adverse conditions for the current imaging system. In our experiments, the average diameter of the tumors was less than 11 mm and the expected elastic contrast was less than 3 [20]. In the case of the two cancers that were missed, their average diameter was less than 6 mm. Overall, sonoelastography detected 7 out of 9 cancers *ex vivo* and 2 out 3 cancers *in vivo*, consistent with previous studies [5].

V.   CONCLUSION

Preliminary results from recent *ex vivo* and *in vivo* studies were evaluated to assess the performance of sonoelastography for prostate cancer detection. Sonoelastographic imaging found 7 out of 9 cancers in the prostate specimens evaluated *ex vivo* and 2 out of 3 cancers from an *in vivo* case. Overall, 3D sonoelastography has shown potential for prostate cancer detection as well as for becoming a guided biopsy tool, albeit based on limited data.
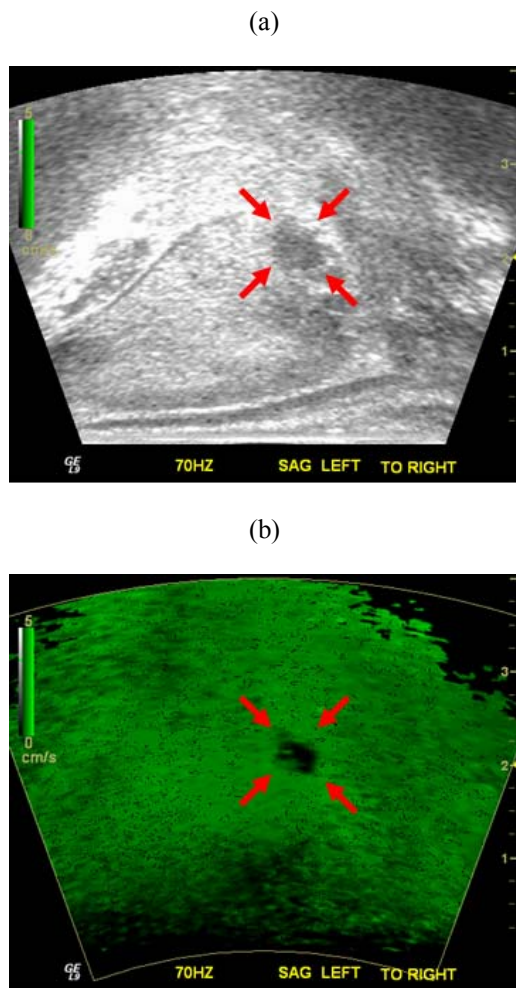
(a)

(b)

Figure 3. Matched (a) B-mode and (b) sonoelastographic images from an *in vivo* scan of the prostate. The sonoelastographic image shows a tumor detected in the center of the image (red arrows).

REFERENCES

[1] American Cancer Society - Cancer Facts and Figures 2007, American Cancer Society, 2007.

[2] A. Reissigl, J. Pointner, H. Strasser, O. Ennemoser, H. Klocker, and G. Bartsch, "Frequency and clinical significance of transition zone cancer in prostate cancer screening," Prostate, vol. 30, pp. 130–135, 1997.

[3] M.C. Benson and C.A. Olsson, "Prostate specific antigen and prostate specific antigen density: Roles in patient evaluation and management," Cancer, vol. 74, pp. 1667-1673, 1994.

[4] W.J. Ellis and M.K. Brawer, "The significance of isoechoic prostatic carcinoma," J. Urol., vol. 152, pp. 2304–2307, 1994.

[5] L.S. Taylor, D.J. Rubens, B.C. Porter, Z. Wu, R.B. Baggs, P.A. di Sant'Agnese, et al., "Prostate cancer: Sonoelastography for in vitro detection", Radiology, vol. 237, pp. 981-985, 2005.

[6] L. Gao, K.J. Parker, R.M. Lerner, and S.F. Levinson, "Imaging of the elastic properties of tissue - A review," Ultrasound Med. Biol., vol. 22, pp. 959-977, 1996.

[7] J. Ophir, S.K. Alam, B. Garra, F. Kallel, E. Konofagou, T. Krouskop, and T. Varghese, "Elastography: Ultrasonic estimation and imaging of the elastic properties of tissues," Proc. Instn. Mech. Engrs., vol. 213, pp. 203-233, 1999.

[8] J. Greenleaf, M. Fatemi, and M. Insana, "Selected methods for imaging elastic properties of biological tissues," Annu. Rev. Biomed. Eng., vol. 5, pp. 57-78, 2003.

[9] A. Lorenz, H. Sommerfeld, M. Garcia-Schurmann, S. Philippou, T. Senge, and H. Ermert, "A new system for the acquisition of ultrasonic multicompression strain images of the human prostate in vivo," IEEE Trans. Ultrason. Ferroelec. Freq. Contr., vol. 46, pp. 1147-1153, 1999.

[10] A. Pesavento, and A. Lorenz, "Real time strain imaging and in vivo applications in prostate cancer," Proc. IEEE Ultrason. Symp., vol. 2, pp. 1647-1652, 2001.

[11] R. Souchon, O. Rouviere, A. Gelet, V. Detti, S. Srinivasan, J. Ophir, and J.Y. Chapelon, "Visualisation of HIFU lesions using elastography of the human prostate in vivo: Preliminary results," Ultrasound Med. Biol., vol. 29, pp. 1007-1015, 2003.

[12] R.M. Lerner, K.J. Parker, J. Holen, R. Gramiak, and R.C. Waag, "Sonoelasticity: Medical elasticity images derived from ultrasound signals in mechanically vibrated targets," Acoust. Imaging, vol. 16, pp. 317-327, 1998.

[13] S.R. Huang, R.M. Lerner and K.J. Parker, "On estimating the amplitude of harmonic vibration from the Doppler spectrum of reflected signals," J. Acoust. Soc. Am., vol. 88, pp. 310-317, 1990.

[14] K.J. Parker, D. Fu, S.M. Gracewski, F. Yeung, and S.F. Levinson, "Vibration sonoelastography and the detectability of lesions", Ultrasound Med. Biol., vol. 24, pp. 1937-1947, 1998.

[15] L.S. Taylor, "Three-dimensional sonoelastography: Principles and practices with application to tumor visualization and volume estimation," Ph.D. Dissertation, University of Rochester, 2002.

[16] H.M. Ladak, F. Mao, Y. Wang, D.B. Downey, D.A. Steinman, and A. Fenster, "Prostate boundary segmentation from 2D ultrasound images", Med. Phys., vol. 27, pp. 1777-1788, 2000.

[17] B. Castaneda, M. Zhang, K. Bylund, J. Christensen, W. Saad, D.J. Rubens, and K.J. Parker, "Semi automatic measurement of thermal ablated lesions in sonoelastography images," J. Ultrasound Med., vol. 26, pp. S87-S88, 2007.

[18] B.C. Porter, "Three-dimensional medical ultrasound acquisition and data registration and fusion," Ph.D. Dissertation, University of Rochester, 2004.

[19] V. Jalkanen, B.M. Andersson, A. Bergh, B. Ljungberg, and O.A. Lindahl, "Resonance sensor measurements of stiffness variations in prostate tissue in vitro - A weighted tissue proportion model," Physiol. Meas., vol. 27, pp. 1373-1386, 2006.

[20] M. Zhang, B. Castaneda, Z. Wu, P. Nigwekar, J.V. Joseph, D.J. Rubens, and K.J.Parker, "Congruence of imaging estimators and mechanical measurements of viscoelastic properties of soft tissues," Ultrasound Med Biol., vol. 33, pp. 1617-1631, 2007.